GEOLOGICA CARPATHICA, 2024, 75, 3, 195–211 https://doi.org/10.31577/GeolCarp.2024.11

Lithospheric scale cross-section through the Transylvanian Basin: A joint geophysical and geological survey

ATTILA NOVÁK[1,2], TIBOR RUBÓCZKI[1,2,3,✉], VIKTOR WESZTERGOM[1,2], MIRCEA RADULIAN[4,5,6], ALEXANDRU SZAKÁCS[1,7], CSABA MOLNÁR[1,2] and ISTVÁN JÁNOS KOVÁCS[1,2]

[1]HUN-REN Institute of Earth Physics and Space Science, Sopron, Hungary
[2]MTA FI Lendület Pannon LitH_2Oscope Research Group
[3]Doctoral School of Earth Sciences, Eötvös Loránd University, Budapest, Hungary
[4]Romanian Academy, Bucharest, Romania
[5]National Institute of Earth Physics, Bucharest, Romania
[6]Academy of Romanian Scientists, Bucharest, Romania
[7]Institute of Geodynamics, Romanian Academy, Bucharest, Romania

(Manuscript received March 20, 2024; accepted in revised form August 8, 2024; Associate Editor: Michal Šujan)

Abstract: The transition area between the Pannonian Basin and the East Carpathians is the subject of considerable tectonic research in Central Europe because of its geological diversity, especially for Lithosphere–Asthenosphere Boundary determinations. The major objective of this study is to investigate the Earth's lithospheric structure and in particular to determine the Lithosphere–Asthenosphere Boundary from the Pannonian Basin, through the Transylvanian Basin to the Carpathian Bend area. We recorded six new deep magnetotelluric soundings and used two archive measurements to complete the information and to put additional constraints on the depth of the Lithosphere–Asthenosphere Boundary. In the part of the discussions we provide a brief overview of the existing various methodologies and Lithosphere–Asthenosphere Boundary determinations for the wider Carpathian–Pannonian region and Europe and comparison with new magnetotelluric results. The lowest Lithosphere–Asthenosphere Boundary depth was detected in the Pannonian Basin (~50 km). Our results indicate in addition that the Lithosphere-Asthenosphere Boundary beneath the Transylvanian Basin (~70–80 km) is not thick and much thinner than those of the European and Moesian Platforms. The additional geophysical information (geomagnetic data and phase tensor results) detected the presence of deep well conductive zones towards the Pannonian Basin, the Bogdan Vodă–Dragoș Vodă fault and the East Carpathians. This could be explained by the elevated position of the well conductive asthenosphere in the Pannonian Basin and deep and presumably fluid rich tectonic zones associated with the Bogdan Vodă–Dragoș Vodă fault and the East Carpathians. The phase tensors highlighted that the most complex tectonic zones are present in the vicinity of the East Carpathians (where the average Lithosphere–Asthenosphere Boundary depth is >100 km), which is in line with the relatively young age of the mountain belt and the very complex nature of collisional orogens.

Keywords: lithosphere, asthenosphere, magnetotelluric soundings, Carpathian–Pannonian Region, Transylvanian Basin

Introduction

There are still relatively few and ambiguous Lithosphere–Asthenosphere Boundary (LAB) determinations for the transitional area between the Pannonian Basin and East Carpathians within the broader Carpathian–Pannonian alpine megastructure of Europe. Depending on the geophysical methods employed, several definitions of the LAB have been proposed (Eaton et al. 2009; Jones et al. 2010). The determination of the lithospheric thickness is complicated because the lithosphere–asthenosphere discontinuity is elusive and imaged with different resolutions by the different geophysical methodologies (Eaton et al. 2009; Karato et al. 2015). Even decades after the birth of the modern plate tectonic theory it is still controversial what causes the observed variations in physical properties at the LAB (e.g., drop in seismic velocity and resistivity). Among many arguments hydrolytic weakening (Girard et al. 2013), elastically accommodated grain boundary sliding (Karato et al. 2015), stress-induced amorphization of olivine grain boundaries (Samae et al. 2021), and the presence of partial melts are the most common proposed explanations (Green et al. 2010; Kovács et al. 2021).

The major objective of this study is to investigate the Earth's lithospheric structure, in particular to determine the LAB along the eastern half of the Carpathian–Pannonian Region (CPR), from the Pannonian Basin to the west, through the Transylvanian Basin to the Carpathian Bend area to the east. To complete the information and to put additional constraints on the depth of the LAB in this geologically complex area, we recorded six new deep magnetotelluric (MT) soundings and used two archive measurements (Harangi et al. 2015; Rubóczki et al. 2024). The cross-section was designed to cover the geo-

✉ corresponding author: Tibor Rubóczki
ruboczki.tibor@epss.hun-ren.hu

logical diversity of the area and try to avoid the immediate vicinity of large faults separating major and minor tectonic units and nappes. The other strict requirement is related to getting reliable measurements over long time intervals. The long-period MT methodology is known to be sensitive to strong conductivity contrast at the LAB, however, it requires a long (~2 weeks) continuous and undistorted time series of magnetic and electric field components to be recorded. Finding suitable sites and ensuring noise-barren recordings is rather challenging. The methodology we follow also enables us to reveal the conductivity distribution in the underlying lithosphere and asthenosphere. This provides a powerful tool to explore whether the different geological units and tectonic settings have different conductivity patterns. In addition, it gives information on the geometry of the well-conducting zones, which can be correlated with geological structures. Thus, we aim to provide new determinations of the LAB depth in the study area and also to reveal if deep lithospheric structures correlate with geological observations and seismicity of the SE Carpathians. We also provide an in-depth comparison to the few already existing LAB determinations for the area using various methodologies and approaches.

Geological background

The Carpathian–Pannonian region (CPR) is situated at the convergence zone between the stable East European Platform (Eurasian Plate) and the Adriatic microplate. The northern and southern part of the CPR is composed of the ALCAPA and Tisza–Dacia lithospheric blocks (microplates) respectively (Schmid et al. 2008; Fig. 1a). During the early Miocene, the eastward movement of the ALCAPA unit was accompanied by a counter-clockwise rotation whereas that of the Tisza–Dacia by a clockwise rotation (e.g., Kázmér & Kovács 1985; Márton 1987; Fodor et al. 1999). These two units are separated by the Mid-Hungarian Shear Zone (MHZ) which is built up by remnants of oceanic lithospheres (Csontos & Vörös 2004; Schmid et al. 2008). The E–W oriented Bogdan Vodă–Dragoș Vodă fault system (Săndulescu et al. 1993; Gröger et al. 2008), representing the eastward continuation of the Mid-Hungarian Shear Zone (Csontos & Nagymarosy 1998), developed during several tectonic episodes including extension (18.5–16 Ma), transpression (16–12 Ma), and transtension (12–10 Ma; Tischler et al. 2007, 2008; Gröger et al. 2008). Its larger inner basin, the Pannonian Basin system, was formed during the Miocene when large-scale extension resulted in considerable thinning of the entire lithosphere, with appreciably less effect on the crust than on the lithospheric mantle. What was the driving force of the extension is still disputed and includes slab-pull exerted on the upper plate during subduction roll-back (Horváth 1993; Horváth et al. 2015); eastward directed asthenospheric flow from the Alpine collision belt (Kovács et al. 2012) and gravitational instability (Houseman & Gemmer 2007). When the roll-back of the subducted slab ceased upon reaching the stable East European Platform, it has resulted in tectonic inversion and gradual shortening of the area in the last 5–10 My (Bada et al. 2007).

The Carpathians is a fold-and-thrust-belt, which began to form in Cretaceous due to the convergence and collision of the European and African plates and several microplates (e.g., Ratschbacher et al. 1993; Linzer et al. 1998). The Transylvanian Basin is the easternmost one among the sedimentary basins. It has a complex evolution history closely related to the formation of the Carpathians and rather different to that of the Pannonian Basin in many aspects (Huismans et al. 1997; Ciulavu et al. 2000), characterized by thicker crust, low surface heat flow, higher average elevations and lack of primary Miocene extensional structures as opposed to the Pannonian Basin (Krézsek & Bally 2006).

Presently, the remnants of the subducting slab or the delaminating lower continental lithosphere can only be detected beneath the Vrancea zone in the south-eastern part of the East Carpathians (e.g. Wortel & Spakman 2000). The Vrancea seismogenic zone in the Carpathian Bend area, adjacent to the SE corner of the Transylvanian Basin, marks the final stage of the convergence process, which is supported and currently expressed by the presence of intensive clustered seismicity there (Wenzel et al. 1999; Radulian et al. 2008; Ismail-Zadeh et al. 2012; Fig. 1). The position of the earthquake hypocenters outlines a steeply NW-dipping fast velocity body seismologically active between approximately 70 and 160 km depth, that is revealed also by the seismic tomography imaging (e.g. Tondi et al. 2009; Ismail-Zadeh et al. 2012). In addition to the active seismic characteristics, the occurrence of volcanic activity during the last ~10 million years along the internal part of the East Carpathians also proves that the Carpathian Bend area is geologically extremely young and still active. The initially calc-alkaline volcanism has changed to high-K calc-alkaline and finally to adakite-like calc-alkaline character, whilst the eruptive centers migrated from Călimani Mountains southward to South Harghita (Pécskay et al. 1995, 2006; Szakács et al. 2018). The last volcanic activity occurred ~30 ka ago at Ciomadul volcano (Harangi et al. 2010; Karátson et al. 2016). The close-by Perşani Mountains is the spot of Na-alkali mafic volcanism which developed between 1.2 and 0.6 Ma at least in five episodes (Seghedi et al. 2004; Panaiotu et al. 2013). The alkaline lavas erupted enclosed upper mantle xenoliths which show fingerprints of intensive deformation and significant metasomatic overprint most probably related to the nearby sinking slab (Vaselli et al. 1995; Falus et al. 2008; Kovács et al. 2018; Lange et al. 2019).

Methodology

The magnetotelluric (MT) geophysical method is based on the time-varying ULF-ELF (Ultra Low Frequency–Extra Low Frequency) geomagnetic field and the response of the imaging of the electrical properties of the Earth (Tikhonov 1950; Cagniard 1953; Ádám 1965, 1976) The penetration depth of the MT method depends on the frequency and quality of

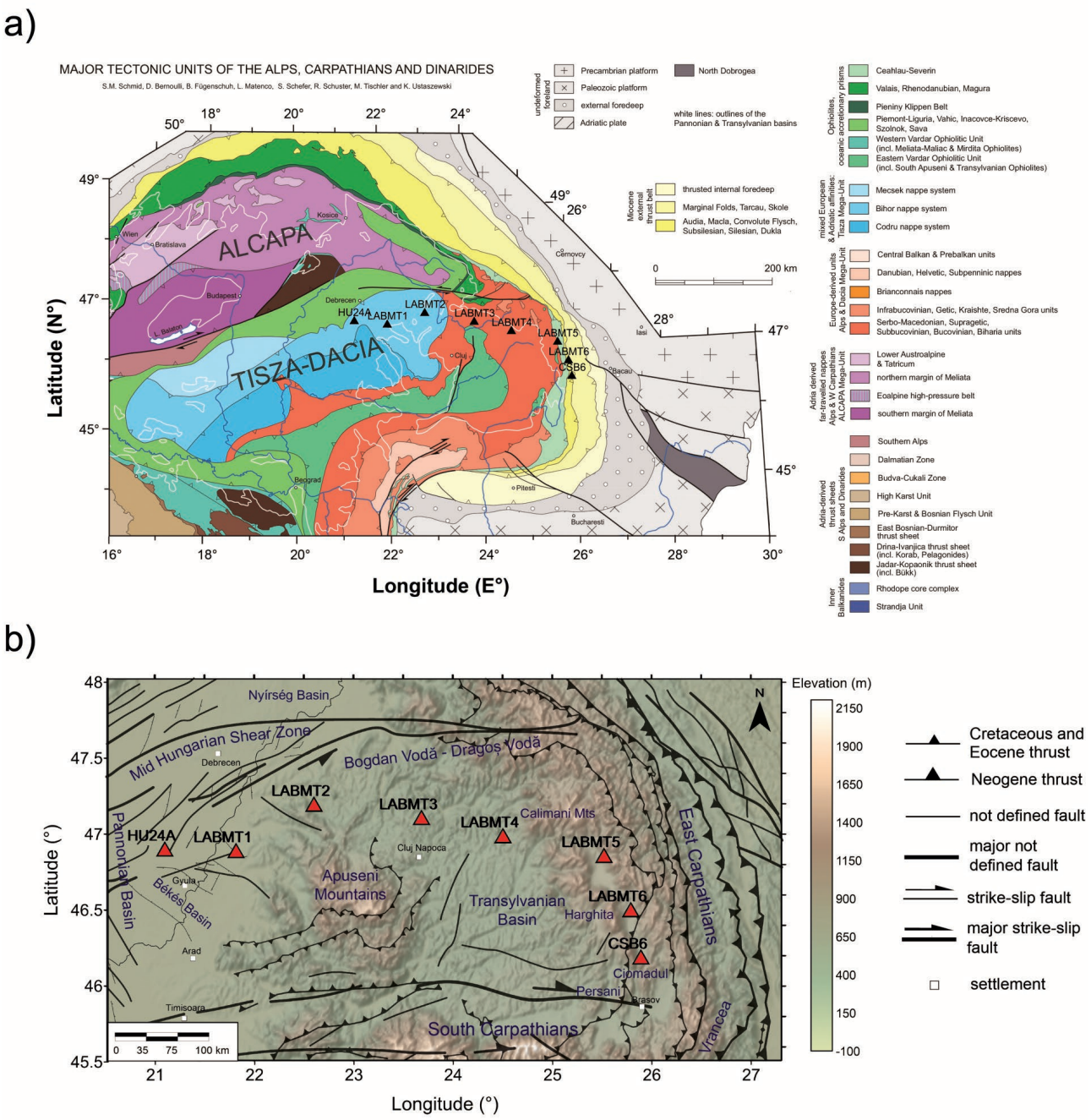

Fig. 1. a — Schematic geological map (based on Schmid et al. 2008) showing the position of the MT stations; **b** — Location of the MT stations on the topographic map in the Transylvanian Basin, with Cretaceous, Eocene and Neogene tectonic elements shown (based on Koroknai et al. 2020 and Tămaș et al. 2021).

the data. The penetration depth can be in the range from a few hundred meters to hundreds of kilometers. The geological information is contained in the magnetotelluric transfer function which provides several quantities of the studied structure by complex surface impedance tensor. The primary information obtained from the transfer function is the period-dependent apparent resistivity and impedance phase of the complex EM field amplitudes.

The fundamental property of the MT method is the sensitivity to resistivity changes which gives an opportunity to study tectonic zones and the whole lithosphere–asthenosphere system. Although the conductivity is controlled by temperature and composition, minor components in the rock matrix such as the presence of an integrated conducting phase (e.g., melt or graphite) play a significant role in processing (Jones 1999; Xu et al. 2000; Ledo & Jones 2005). The MT method is well

suited to the determination of the LAB position, as this is characterized by a significant difference between the conductivity of the lithosphere and the asthenosphere. Typical resistivity values of the well conductive asthenosphere are in the range of 1–25 Ωm for a continental plate (Heinson 1999; Jones et al. 2010). During the data processing, we assumed that the indication of the asthenosphere is either when the resistivity decreases to these values or when resistivity decreases by at least an order of magnitude. Accordingly, the electrical lithosphere–asthenosphere boundary (eLAB) was considered as the bottom layer of the simple layered MT model for the inversion.

Field campaign and data processing

In the TopoTransylvania project (Matenco 2018) field campaign we installed six broadband MT stations along a roughly E–W directed profile from the Pannonian Basin, through north of the Apuseni Mts. to the Carpathian Bend area across the Transylvanian Basin (Fig. 1b). Two former stations were integrated into the network (HU24A and CSB6) where the average distance between the stations was approximately 100 km. MT data acquisition implemented high frequency (LEMI-419) and long-period (LEMI-417) signal recorded to achieve broadband MT periods between 10^{-2} s to a few 10^{4} s. During the field MT deployment in Transylvania in 2018, ensuring anthropogenic noise-free conditions as a minimum requirement for the electrical infrastructure, 5–10 km distance from the electric power grid was fulfilled for all station locations. In all cases, the duration of the long-period measurements was exactly 2 weeks, which was sufficient to obtain reliable response functions at 10^{4} s.

The time series were processed using robust single-site EMTF code to estimate the MT transfer functions (Egbert & Booker 1986; Egbert & Livelybrooks 1996). 48 frequency bands were selected where the coherency condition of the electric and magnetic field components was 95 percent for both systems. The apparent resistivity and the phase were calculated from the estimated transfer function (impedance). To eliminate the galvanic distortion effects from the soundings we used the Groom-Bailey decomposition (Groom & Bailey 1989). Due to data quality and noise, some frequencies were masked from the soundings (i.e., in the case of the LABMT5 station the high-frequency range was not available). The TE and TM modes of the decomposed MT soundings fit well together in all cases, in addition the initial soundings contained little static shift, therefore we did not separately apply a static shift correction on the MT data. The decomposed MT soundings formed the basis of the inversion process (Supplementary Fig. S1).

Even though the stations are located along a section, we decided that the best method to adopt for this investigation is the 1-D inversion method, because the distance between MT stations was too large (100 km in average) to obtain a consistent result from 2-D inversion. To establish whether a decrease in resistivity occurs to the expected value marking the LAB the 1-D inversion technique is well suited. 1-D inversion was calculated by the WinGLink (GEOSYSTEM SRL 2008) software package by the decomposed invariant data to determine the resistivity and layer thickness of the geological model. The starting model was estimated by Occam's inversion (Constable et al. 1987) and used both the amplitude and the phase values to fit the measured data. Different number of layers adjusted to the inversion considering the raw data. The RMS (root mean square) misfit was minimized for the layered inversion where the average values do not exceed 0.15 percent. The fitting of the 1D MT inversion models to the decomposed soundings in invariant mode for the apparent resistivity and the phase is shown in Supplementary Fig. S2.

In this study, we used two common tools to extract structural information from MT data: geomagnetic induction vectors and phase tensor ellipses created by the MTPy code (Kirkby et al. 2019). The Geomagnetic Transfer Function (also known as the tipper vector or induction arrows) is a dimensionless complex vector. It is defined as the relation between the vertical and the two horizontal components of the magnetic field. It contains information on the presence of lateral variations in conductivity by representing a projection of the vertical magnetic field on the horizontal xy plane. The vectors correspond to its real and imaginary parts where the real vectors are called induction vectors. In this paper, we applied Parkinson's convection where the real induction arrow points toward concentrations of current as more conductive zones (Parkinson 1959; Wiese 1962).

The phase tensor analysis, based on Caldwell et al. (2004) and Bibby et al. (2005), creates an opportunity to investigate the geoelectric direction and dimension of the subsurface resistivity distribution free of the galvanic distortions. This can be graphically represented with an ellipse and describe the dimensionality of the structure by the elongation and the β skew angle. If the ellipse forms a circle, it means a purely 1-D resistivity structure. When the circle is transformed into a rotated and elongated ellipse, characterizing different (strike or non-strike elongated) 2-D structures. The general 3-D case is represented by increasing values of the β skew angle.

Results

The apparent resistivity and phase of the MT soundings in the Transylvanian Basin MT section are continuous, trend-like points in TE and TM modes also (Supplementary Fig. S1). After applying Groom-Bailey tensor decomposition, the difference between TE and TM modes almost disappeared, and 1D inversion processing, in their invariant mode, was performed using 1-D Occam and simple layered inversions approaches. The 1-D inversion results of the new MT stations in the Transylvanian Basin are summarized in Fig. 2. The layered models show the resistivity distribution at depths down to 125 km, where in the upper 25 km the inversion models introduce a variety of crustal structures with different resistivity

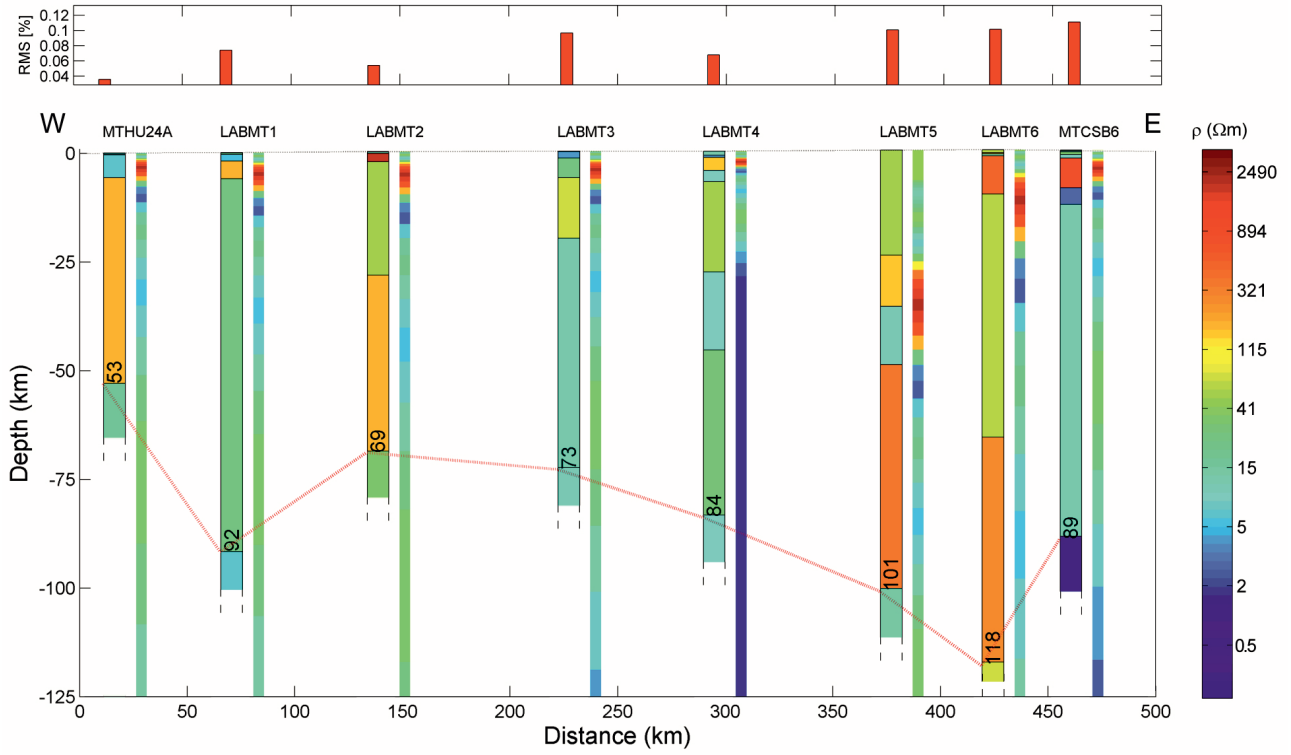

Fig. 2. 1-D layered and OCCAM (narrow column) inversion results of MT data with RMS (nRMS, layered inversion) values along the W–E profile. The red line represents the LAB depth with calculated values of 1-D layered inversion.

layers. The shallow lithosphere heterogeneity is characterized by many resistive features (10 to ~2000 Ωm) embedded within a highly resistive background formation. The MT inversion models do not show any resistivity contrast between the lower crust and the lithospheric mantle, thus there is no evidence for the electric Moho along the investigated section in the Transylvanian Basin. However, from the seismological S receiver function analysis carried out by Kind et al. (2017), there is Moho depth estimation in the Transylvanian region. In the deep lithosphere, the MT measurements mostly show higher resistivity (>100 Ωm) in the upper mantle. The thickness of the lithosphere can be deduced from the MT layered inversion models by delimiting the depth at which transition occurs from the higher resistive lithosphere to the more conductive asthenosphere. A significant well-defined trend is manifested for the suspected resistivity changes from which the LAB can be identified. At the western part of the MT profile, close to the border of the Pannonian Basin, a typically shallow LAB depth (~60 km) is indicated with correlation to the early MT LAB depth map by Ádám & Wesztergom (2001). From the Pannonian Basin towards the Transylvanian Basin, the LAB depths increase (Fig. 2). Further to the direction of the Transylvanian Basin the LAB depth moderately decreases, and then towards the East Carpathians has a higher value again (~120 km). Approaching the Carpathian Bend area including the Ciomadul Volcano (CSB6), the estimated LAB depth has a substantial change to a lower value (~90 km).

The induction arrows are shown on a horizontal topography map of the Transylvanian Basin in Fig. 3 with six selected frequencies. The horizontal maps cover the range between 1 s to 3277 s periods which correspond to shallower and greater depths, respectively. At the lower period (1 s) the induction arrows at the stations of LABMT1, LABMT2, and LABMT4 pointed to the central part of the Transylvanian Basin, otherwise the arrows represent crustal discontinuities. The stations located near the East Carpathians turn to the east direction. From the 85 s period, the higher magnitude (length) of induction arrows is indicated at LABMT1 and LABMT2 stations, where the vectors point to the north-northwest direction towards the Pannonian Basin. The magnitude of the induction arrows decreases with depth and slowly turns to the north. The induction arrows at the center of the profile represent an eastern direction which changes with depth to the northeast. In the East Carpathians, the induction arrows show significant south-southeast direction, and these characteristics can be followed to larger depths with a gradual inflexion towards the east.

The phase tensor ellipses show variable shapes with nearly zero β skew angles at short periods, except LABMT3. At longer periods, at 85 s and 341 s, the ellipses are separated into three segments represented by the color of the skew angles, where at longer periods these values change to the positive range. In other periods, the shape of the ellipses shows no significant changes, except for three stations (LABMT5,

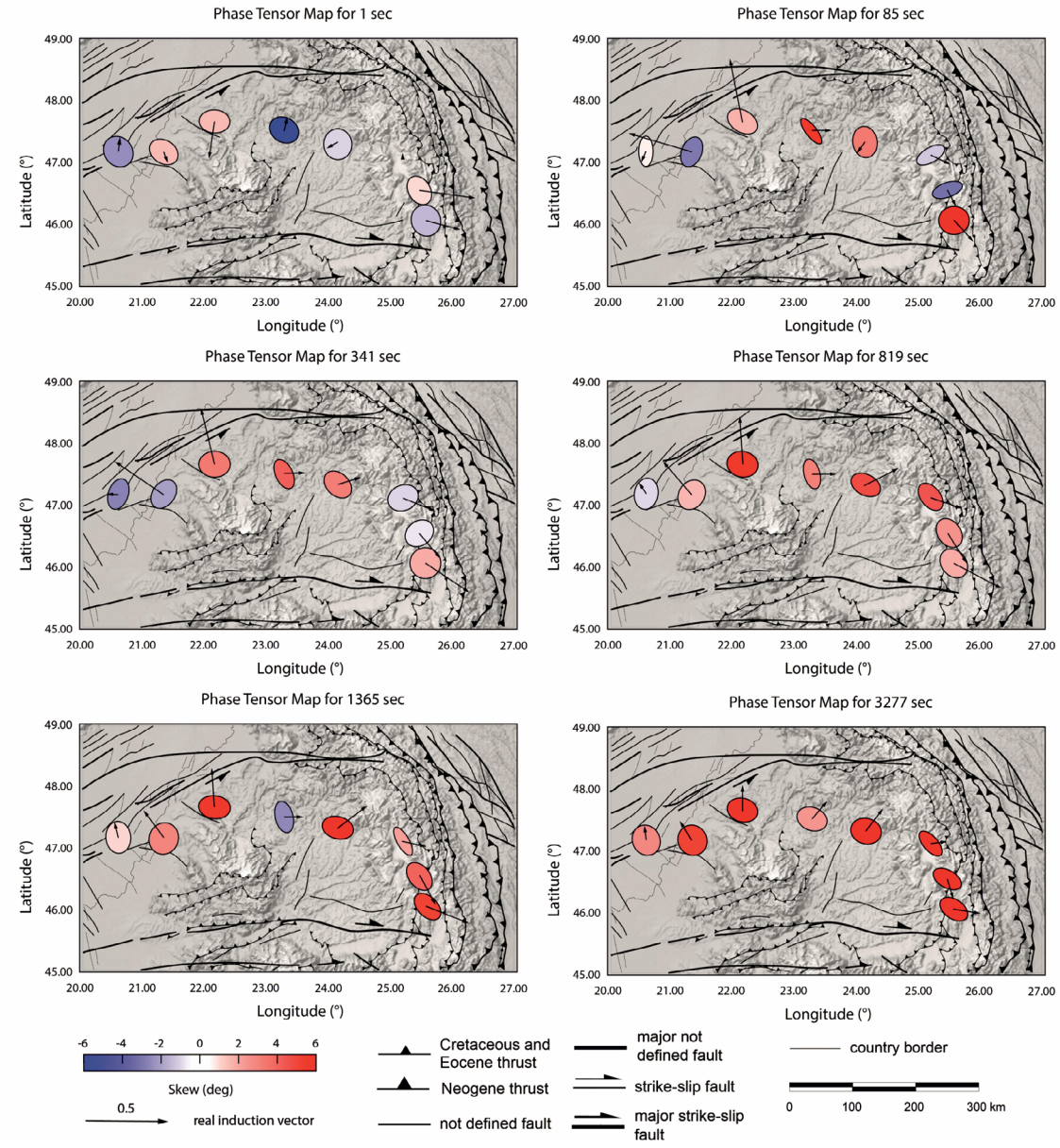

Fig. 3. Induction arrows and phase tensor ellipses at six selected frequencies (depth) shown on the topography map and represent structures of Cretaceous, Eocene and Neogene faults based on Koroknai et al. (2020) and Tămaș et al. (2021). The ellipses are colored based on the β skew angle.

LABMT6, MTCSB6) having a slight change in the elongation from the north-northeast to the east. In the case of the East Carpathian MT stations, the phase tensor ellipses reveal an increasing skew with depth, implying a more complex local 3D geological structure than in the Transylvanian Basin.

LAB determinations in the wider Carpathian–Pannonian Region

The first LAB determinations in the Carpathian–Pannonian region were performed using seismological (Babuška et al. 1987; Babuška & Plomerová 1988), later magnetotelluric (Praus et al. 1990; Horváth 1993; Ádám et al. 1996), and geothermic (Čermak 1993) data. We must note, however, that the obtained LAB determinations by these different geophysical methodologies disagree up to 50–60 km in some areas. These various methodologies and approaches have their pros and cons. In this part of the discussions we provide a brief overview of the previously applied methodologies and LAB determinations for the wider CPR and Europe.

Thermal approach

While traditionally the ~1300 °C isotherm was used to define the base of the rheologically strong lithosphere (McKenzie

1978), later studies proposed lower temperatures. In their pioneering paper Pollack & Chapman (1977) proposed that the LAB coincides with the depth where the temperature exceeds 85 % of the dry solidus, which usually equals to 1100–1200 °C in most tectonic settings. The widely adopted thermal definition considers the lithosphere as a layer in which heat transfer occurs prevalently by conduction and is rheologically strong at lower temperature than these critical values. There are, however, contrasting views on what happens at these temperatures which explain the obvious contrasts in the physical properties. This could only be a temperature-dependent physical transformation such as melting, dehydration, changing deformation mechanisms or storage capacity of volatiles in minerals (e.g., Artemieva 2009; Eaton et al. 2009).

It was Stegena et al. (1975), who first suggested that the thin lithosphere and high heat flow in the Pannonian Basin are related. Royden et al. (1983) show that the heat flow and the subsidence of the Pannonian Basin may be explained by non-uniform thinning of the lithosphere. To model the high heat flow and high post-rift subsidence rate they assume that the mantle part of the lithosphere was almost completely thinned. The average lithospheric thickness in the Pannonian Basin is 60 km, therefore we assumed in our present paper that heat flow variations caused by changes in the lithospheric thickness had the same, or even larger, wavelength. Tesauro et al. (2009) assumed that the LAB coincides with the 1200 °C isotherm, and they found that the lithosphere becomes thicker, up to 120–140 km toward the flanks of the Pannonian Basin, beneath the Bohemian Massif and the Alpine foredeep and to ~150 km beneath the Carpathians.

The thermally defined lithosphere is systematically thicker than the electrical, petrologic and seismic lithosphere (Dérerová et al. 2006; Tesauro et al. 2009; Tiliță et al. 2018) and is comparable with the lithosphere thickness evaluated by isostasy (Artemieva & Shulgin 2019). Kovács et al. (2017) modeled the depth of the 1050 and 1100 °C isotherms beneath the Pannonian Basin and found it at typically shallower than 90 km depth but more commonly at ~60 km depth. It was only deeper where the real heat-flow was underestimated due to the cooling effect of karst water (e.g., Transdanubian Central Range, Bükk Mts., Mecsek Mts.). These isotherms at 1050 and 1100 °C correspond to the pargasite dehydration solidus (Green et al. 2010; Kovács et al. 2021) of the upper mantle, which separate the melt-barren and melt-bearing parts of the upper mantle: the lithosphere and the asthenosphere. A similar approach was adopted by Niu & Green (2018) in estimating the depth of the LAB beneath oceanic basins where it is equated also with the 1100 °C isotherm.

Seismic determination of the LAB

Shear wave Receiver Functions (SRF)

A shear wave velocity drop of 2–10 % is usually associated with the LAB which could be due to several different reasons including the presence of partial melt in the asthenosphere (Thybo 2006; Saha et al. 2018), changes in deformation creep mechanisms (diffusion and dislocation creep, Fei et al. 2016; Aulbach et al. 2017), or an elevated water-containing layer produced by fluid metasomatism (Aulbach et al. 2017). Elastically accommodated grain boundary sliding (EAGS) can also explain the lower seismic velocities at the LAB (Karato 2012). Jackson et al. (2010) experimentally constrained a presumably EAGS-triggered relaxation peak (at 1 Hz) at ~1050 °C for dry and melt barren upper mantle rock with ~1 mm grain size. This suggests that the seismic velocity decrease could also be accounted for without evoking partial melting at temperatures which are usually assumed in the vicinity of the LAB. In accordance, Samae et al. (2021) proposed that grain boundary sliding could be intensified at the glass transition temperature of amorphous olivine, which could decrease the viscosity and seismic velocity at the LAB. The glass transition temperature of amorphous olivine is in the temperature range of 1050–1150 °C typically which, in turn, occurs at geophysical anomalies usually associated with the LAB (Pollack & Chapman 1977; Samae et al. 2021).

The velocity reduction of seismic waves at the LAB can be detected by several different methodologies especially for the shear waves. This velocity reduction at the LAB creates a negative phase on the receiver functions the depth of which, the negative phase depth (NPD), could be equated with the LAB in several geotectonic settings (e.g., Abt et al. 2010; Kalmár et al. 2023).

The Carpathian–Pannonian region was partially involved in the first European SRF study of Geissler et al. (2010), which provided LAB estimates for 4 stations in the Pannonian Basin: PSZ (~101 km), BUD (~74 km), SOP (~89 km), and PKSM (~103 km). Another previous SRF study of Klébesz et al. (2015) in the northern Hungarian region (e.g., PSZ station) determined a LAB depth of 65 km (±10 km). Kind et al. (2017) provided a few 2D common conservation point (CCP) migrated cross-sections in the Pannonian Basin region. These NPD values are ~60–80 km in the Pannonian Basin (shallow lithosphere) and also in the South and East Carpathians (>90 km; thicker lithosphere), where the depth values most likely do not indicate the LAB.

More recently Kalmár et al. (2023) have constructed an NPD map based on 1D migration data from 389 seismological stations using the natural neighbor interpolation scheme (Sibson 1981). Their NPD determinations in the CPR bear smaller uncertainty (±6 km) than previous studies and seem to coincide well with the other LAB determinations for the central part. Accordingly, the Pannonian Basin is characterized by a thin lithosphere (~60 km), associated with high surface heat flow (>90 mW/m^2, Lenkey et al. 2021). In the areas where the lithosphere is thicker (>90 km) and the surface heat flow is lower (<70 mW/m^2), NPD values obtained from 2D CCP migration are less likely consistent with the LAB, but is probably indicative of another shallower intra-lithospheric discontinuity (also referred to as the mid lithospheric discontinuity – MLD – in other studies (e.g., Kind et al. 2017; Rychert et al. 2020).

Kalmár et al. (2023) determined ~64 km LAB depth for the PSZ station in northern Hungary resembling closely that of Klébesz et al. (2015), but with only ±4 km absolute uncertainty due to the larger, quality-controlled data set and considerably improved data processing routine. Belinić et al. (2018) studied the Dinarides and its vicinity and implemented 1D migration using the IASP91 velocity model. The LAB depths determined for the southwestern part of Hungary (~65 km), in the foreland of the Eastern Alps (~100 km) and in the Northern Dinarides (~80 km) resembles closely the estimations of Kalmár et al. (2023).

Seismic tomography

Seismic tomography reveals the velocity distribution of seismic waves, where the LAB can be equated with the location of a velocity drop below the MOHO in the upper mantle. Plomerová & Babuška (2010) conducted one of the first global tomographic studies to determine the depth of the LAB in the CPR. The authors concluded that in areas with thick sedimentary cover, such as the Great Hungarian Plain and the Vienna Basin, the LAB is located at a depth of ~70 km. For the surrounding orogens, this European-scale model provides LAB values of ~125 km. Several other regional seismic body wave tomography investigations were undertaken providing information on lateral variation of the lithospheric structure. The inversion using teleseismic data cover the upper mantle depth range over the entire CPR (Ren et al. 2012) and the Carpathians Bend area (Martin & Wenzel 2006), while the inversion using local data is restrained to the area situated just above the Vrancea intermediate-depth seismic source (Popa et al. 2005; Russo et al. 2005; Baron & Morelli 2017). All these studies outline the presence of an anomalous low-velocity body in the NW part of the Carpathian Bend interpreted as an upwelling of the asthenosphere material following a detachment/delamination process in the lithosphere.

Seismic anisotropy

Babuška & Plomerová (1992) and Plomerová et al. (2002b) defined the LAB as the depth where the direction of seismic anisotropy switches from a lithospheric 'fossil' direction to an asthenospheric plate-flow direction parallel to absolute plate motions. This change in anisotropy can be mapped by the azimuthal variation of P-residuals. The authors found that the LAB topography shows a broad lithospheric thinning beneath the Pannonian Basin. Detailed modelling of the LAB across the Trans-European Suture Zone (TESZ) towards Fennoscandia reveals a stark variation at the boundary marking the base of individual mantle lithosphere blocks with contrasting anisotropy pattern (Plomerová et al. 2002a; Babuška & Plomerová 2004). The LAB shallows only to ~60 km beneath young extensional European basins but deepens to ~220 km beneath the Alps and the South Carpathians and eastward of the Trans-European Suture Zone (TESZ).

Previous MT LAB depth estimations

The eLAB is traditionally identified by a rapid reduction in electrical resistivity (i.e., rapid increase in electrical conductivity) in the shallow upper mantle (Heinson 1999; Jones 1999). The asthenosphere has low resistivity, with global variations in the range of 1–25 Ωm (Heinson 1999). Sensitivity tests revealed that with modern, high quality MT data (errors <2 % in impedance) the onset of the asthenosphere can be detected with a precision of better than 10 % (Jones 1999). The contrast between the lithosphere and the asthenosphere could be due to several reasons. The higher conductivity could be explained by the elevated structural hydrogen concentration incorporated in nominally anhydrous minerals (NAMs; Fullea 2017), which enhances the proton conduction under physical conditions of the upper mantle, where the contribution of ionic and polaron (i.e., ferric vs. ferrous iron) conduction becomes limited (Selway et al. 2014).

Conductivity could also be enhanced by the presence of hydrous minerals such as pargasite and phlogopite (Selway et al. 2015) and the presence of partial melts, where carbonate melts have higher conductivity than silicate melts (Sifré et al. 2014). Note that while elastically accommodated grain boundary sliding, grain boundary amorphization, decreasing grain size and changing deformation mechanisms (i.e., different anisotropy) could explain the temperature dependency of the LAB, and the decrease of seismic shear waves in particular, these mechanisms, however, have limited capacity to explain the very steep resistivity reduction associated with the LAB. Out of these suggested explanations for the origin of the LAB partial melting, increased volatile and hydrous mineral contents in the upper mantle seem to account better for variations of all physical properties at the LAB.

Korja (2007) investigated the LAB depth beneath Europe based on electrical conductivity estimated with magnetotelluric methods. Similar studies have been conducted in the Pannonian region for a long time (Ádám et al. 1996; Ádám & Wesztergom 2001), but the identification of the exact LAB depth has been challenging because the determinations varied in a relatively wide zone (~45–90 km) in the extensional Pannonian Basin having a thin lithosphere.

Joint interpretations for the LAB

Horváth (1993) presented a joint identification of the LAB based on seismic, seismologic and magnetotelluric data. His determination, which is in part also based on the studies of Babuška & Plomerová (1988, 1992, 1993), shows that the Pannonian Basin is characterized by thin lithosphere (~60 km) and crust (~25 km). In contrast, the mountain arc around the basin system has a deep root with thick crust and lithosphere. Posgay et al. (1995) was among the first identifying reflections bouncing back from the LAB by active seismic surveys. The Pannonian Geotraverse (PGT) deep reflection seismic profiles clearly reveal the presence of a thin, attenuated crust and lithosphere in the Pannonian Basin. Along the PGT lines

the MOHO and LAB depths are generally around 25 and 60 km respectively, but under the Békés Basin (SE part of the Pannonian Basin) the depth to the MOHO is slightly less than 22 km, whereas the thickness of the lithosphere is approximately 40 km. Incorporating these results and complemented with gravity and heat flow data Tari et al. (1999) refined further the lithospheric structure in the Pannonian Basin.

Bielik et al. (2022), based on Dérerová et al. (2006), also presented an integrated study on the lithospheric structure and thickness in the Carpathian–Pannonian region. The lithosphere thickness shows noticeable variations across the orogen, as well as along the strike of the Carpathians. The depth of the LAB varies from 240 km in the East Carpathians to 75–110 km, under the Pannonian Basin. Along the Carpathians, the lithospheric thickness increases from the west (~100 km) to the east (~240 km). The South Carpathians shows a ~180 km thick lithosphere.

Discussion

LAB determinations for the study region in the context of the new MT results

The new eLAB depth estimates from the TopoTransylvania MT section are compared to the LAB definitions presented in the previous chapter from the Pannonian Basin through the Transylvanian Basin to the East Carpathians on Fig. 4. In general the TopoTransylvania MT eLAB values in the Pannonian Basin and the western part of the Transylvanian Basin are in good agreement with the results obtained using most of the methods. The LAB depth, constrained by the position of the 1200 °C isotherm (Fig. 4a; Tesauro et al. 2009) and a P-residual study (Fig. 4c; Plomerová & Babuška 2010) indicates increasing deviations from the eLAB towards the East Carpathians. This means that while the LAB depth agrees well from the Pannonian Basin it is even 50 km thicker towards the stable European Platform as seen by the geothermal and seismic anisotropy. Similar significant differences are observed for the LAB defined by seismic anisotropy (see Fig. 4d; Plomerová et al. 2002a, 2006; Babuška & Plomerová 2006; Jones et al. 2010) showing increasing discrepancies towards the East Carpathians. For these three previous cases (Fig. 4a, c and d) the larger discrepancy lies in the resolving power of the applied methodologies and also poor areal coverage of the input geophysical dataset. The best agreement is seen with the negative phase depth (NDP) obtained from S-to-P receiver functions (Fig. 4b; Kalmár et al. 2023) for most of the study area and higher discrepancies are only observed along the East Carpathians. This may be due to the fact that receiver functions in some cases may not be effective enough in detecting the LAB. The highest challenge is how to separate the arrivals directly from the LAB from the multiple converted phases from the Moho discontinuity. Especially in complex tectonic areas such as the Carpathian Bend area, where present-day active geodynamic processes are very intense, the signals coming from LAB could be hidden and hard to extract from RF diagrams (Geissler et al. 2010; Kind et al. 2017). In such cases, the LAB signal may be probably disturbed by the complicated structure due to extrusion, slab roll-back and the possible delamination of the continental lithosphere. The fit is also really good to the combined LAB map by Tari et al. (1999) and Horváth (1993) (Fig. 4f). Both the absolute depth of the LAB and also its variation closely resemble. There is, however, a significant discrepancy to Bielik et al. (2022) as our eLAB depths are significantly smaller and show less steep increase towards the European Platform (Fig. 4g).

The eLAB estimations by Jones et al. (2010) based on Korja (2007) at their stations located in the East Carpathians and Pannonian Basin, show similar values in the Pannonian Basin and the Transylvanian Basin (Fig. 4e). Their results, however, differ significantly in the Carpathians. Detailed magnetotelluric studies were also carried out in the study region along Carpathian Bend by Stănică (1993) and Stănică et al. (1999), some of them were only shorter period soundings unable to achieve higher skin depth reaching the LAB. However, the wide band soundings resulted shallower lithospheric lid (80–100 km) in the younger Transylvanian Basin, and surrounding old platforms the estimated depths were over 150 km (Stănică 1993). These studies, in addition, determined well conductive zones at ~10 km depth along the Carpathians.

Figure 4h summarizes and compares the different LAB determinations. All show increasing LAB depth towards the East Carpathians, and thicker but still not thick lithosphere below the Transylvanian Basin (~80 km). Our eLAB determination shows some increased LAB depth at the transition between the Pannonian Basin and the Transylvanian Basin close to the Apuseni Mts. Including our LAB determination the results of Tesauro et al. (2006) and Bielik et al. (2022) indicate thinner lithosphere in the Carpathian Bend area, which will be discussed further below. In summary, our high quality and spatially better resolved TopoTransylvania MT section indicates ~70–80 km thick eLAB beneath the Transylvanian Basin and thinning in the Carpathian Bend area. Therefore, it is more likely that the lithosphere is thinner under the Transylvanian Basin as it is inferred by other studies and methodologies.

Induction arrows and phase tensors

The determined induction arrows and phase tensors along the TopoTransylvania MT section (Fig. 3) seem to be in line with the broad geological structure of the area. Induction arrows point toward well conductive zones in the lithosphere. At shorter periods up to 341 s (i.e., shallower depths) the induction arrows show a scattered pattern while at longer periods a consistent pattern seems to emerge. The stations in the vicinity of the Pannonian Basin point towards N-NW, which roughly points towards the Pannonian Basin as a well conductive zone. The good conduction could be explained by the elevated position of the well conductive asthenosphere beneath the Pannonian Basin (e.g., Ádám et al. 2017; Kovács

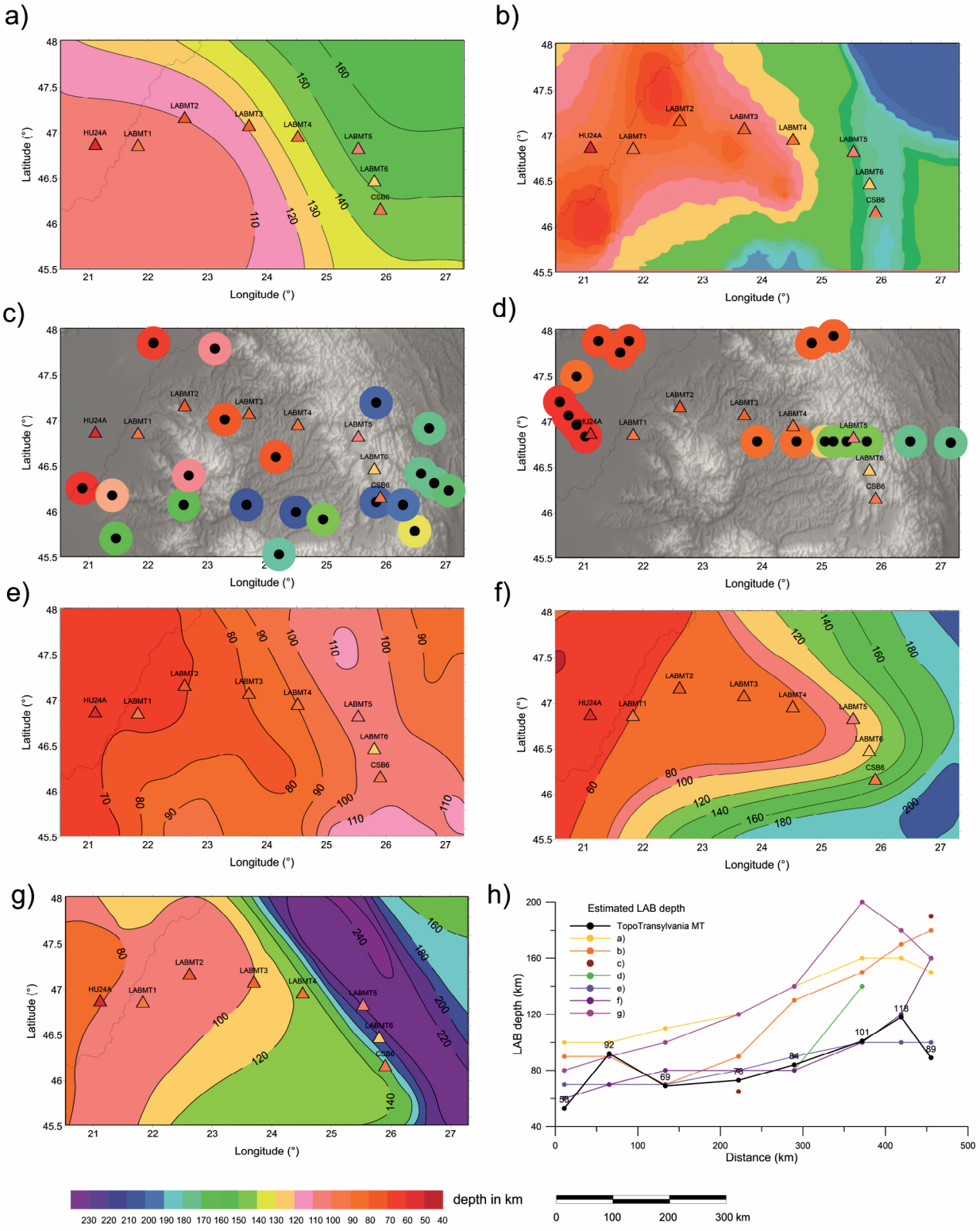

Fig. 4. Compared the MT results of LAB depth estimation on different geophysical and geochemical results: **a** — depth of the isotherm of 1200 °C marking the lithosphere-asthenosphere transition as in fig. 5 of Tesauro et al. (2009); **b** — NPD map from 2-D CCP migration based lithospheric thickness map results in fig. 9 by Kalmár et al. (2023); **c** — LAB depths derived in fig. 2 of P-residual study by Plomerová & Babuška (2010); **d** — Estimates of the depth to the seismic anisotropically defined LAB in fig. 2 of Jones et al. (2010) and references therein: (Babuška & Plomerová 2006; Plomerová et al. 2002a, 2006); **e** — Estimates of the depth to the electrically-defined LAB (eLAB) in fig. 6 by Jones et al. (2010) and Korja (2007); **f** — Lithospheric thickness based on seismologic and magnetotelluric data by Horváth (1993); Tari et al. (1999, fig. 7); **g** — combined map of LAB depth estimation based seismological, magnetotelluric and geothermic data by results in fig. 9 by Bielik et al. (2022); **h** — statistical diagram of LAB depth distribution over distance by different estimation.

et al. 2021). Towards the east, also at longer periods, the induction arrows gradually turn clockwise into E-SE direction. In those directions there is first the primary Bogdan Vodă–Dragoș Vodă fault which separates the ALCAPA and Tisza–Dacia Microplates on the north. This tectonic zone could be considered as the eastern continuation of the Mid-Hungarian Shear Zone. Rubóczki et al. (2024) demonstrated that a deeply penetrating well conductive anomaly is present along the Mid-Hungarian Shear Zone which is due to the presence of fluids or well conductive rocks. It is likely, therefore, that similar deep well conductive zone is expected to occur also along the Bogdan Vodă–Dragoș Vodă fault. More to the east along our TopoTransylvania MT section, close to and along the East Carpathians the induction arrows point towards the East Carpathians and the Carpathian Bend area. Since subduction operated along the East Carpathians and it recycled significant amount of volatiles back to the upper mantle, which resulted in a significant geochemical refertilisation along the orogeny, which also lead to arc-like volcanism since the Miocene (Szabó et al. 1992; Seghedi et al. 2004). The presence of fluids along these very deep subduction structures could create extensive well conductive zones, which explains the direction of induction arrows along the East Carpathians.

At periods between 85 s and 341 s, the ellipses are separated into three segments by color (skew angle) representing the different geological structure of the Pannonian Basin, the Transylvanian Basin and the Carpathian Bend area. The phase tensors display also consistent pattern at longer periods clearly indicating the presence of very complex resistivity structures along the East Carpathians, but less complex structures towards the Pannonian Basin. This could be explained by the very young and complex geological structures along the orogen and in the Carpathian Bend area.

Asthenospheric updoming attenuation – to the Transylvanian Basin

Our eLAB determinations indicate shallower LAB in the Carpathian Bend area. This result could be in line with the identified asthenospheric upwelling adjacent to the Vrancea slab, already demonstrated in several previous studies (e.g.; Russo et al. 2005; Martin & Wenzel 2006; Ren et al. 2013; Petrescu et al. 2020). Figure 5 shows a summary of these key observations. Along section A–A' Popa et al. (2012) performed a detailed local seismic tomography study and identified vertically-extended low velocity anomalies in the Carpathian Bend area under the Ciomadul and Perşani Mts in particular (Fig. 1). In their B–B' N–S oriented cross section Kind et al. (2017) demonstrated the presence of a significant negative velocity anomaly in the Carpathian Bend area from ~150 km to ~50 km depth by using S receiver functions.

Along the C–C' section Russo et al. (2005) studied the seismic attenuation (i.e., spectral ratio analysis) in the Carpathian Bend area and revealed strong attenuation of seismic waves under this region. Among the possible geological interpretations the authors proposed that an asthenospheric dome could exist roughly between the surface suture zone of the Carpathians and the Vrancea seismogenic body. Ren et al. (2012) implemented P-wave finite-frequency teleseismic tomography in the Carpathian-Pannonian region. Their results while characterized uneven quality along section D–D' in the study area, still indicate the presence of a slow seismic velocity anomaly in the Carpathian Bend area.

Tiliță et al. (2018) investigated the thermal structure of the lithosphere in the Carpathian Bend area along section E–E'. The authors find that the high temperature isotherms (i.e., 1300 °C) are at shallower position in the area and appear to spatially coincide with low velocity anomaly revealed by the tomographic study of Martin & Wenzel (2006).

In summary, all these prior observations and our results demonstrate the presence of an anomaly in the Carpathian Bend area characterized by higher electrical conductivity, lower seismic velocity, higher attenuation of seismic velocity and higher temperature. The most straightforward interpretation is the presence of a regional scale asthenospheric updoming. There are several key geological phenomena in the area which could be the consequence and related to this regional asthenospheric upwelling. A striking feature of this area is the very young volcanic activity with the latest volcanic eruptions of the Ciomadul Volcano just ~30 kyrs ago (Szakács et al. 2018; Karátson et al. 2019; Molnár et al. 2019). Similarly, alkaline basaltic volcanic activity in the Perşani Mts. ceased just a few hundred kyrs ago in roughly the same area (Pécskay et al. 2006; Szakács et al. 2018). The Carpathian Bend area is also known for its CO_2 rich gas emanations and carbonated springs which also could be due to the volatiles originated from the asthenosphere and raising towards the surface (Kis et al. 2019; Lange et al. 2023). The source of the volatiles could be the melt bearing and continuously degassing asthenosphere, where volatiles could come to the surface through deep deformation zones along the East Carpathians (Kovács et al. 2021). The Carpathian Bend area is characterized by very complex geodynamics as this is the youngest part of the Carpathians and the segment of the mountain chain emerged only in the past few million years (Leever et al. 2006). The Carpathians could be characterized by active raise, whereas the adjacent Focsani Basin to the east displays very intensive recent and ongoing subsidence (Leever et al. 2006). Upper mantle xenoliths from the young alkaline basalts of the Perşani Mts. show signs of intensive deformations (Falus et al. 2008; Kovács et al. 2018; Lange et al. 2019, 2023), which could be related to this active deformation of the area affecting the upper mantle as well. Our new eLAB determinations demonstrated the elevated position of the well conductive asthenosphere in the Carpathian Bend area with respect to other parts of the Transylvanian Basin.

The question arises what could cause this asthenospheric upwelling in the Carpathian Bend area. A geologic model was presented by Liptai et al. (2022) and Kovács et al. (2021). Both papers argued that there is an 'asthenospheric jam' in the Pannonian Basin and the low viscosity asthenosphere is squeezed between the thicker Adriatic and European plates

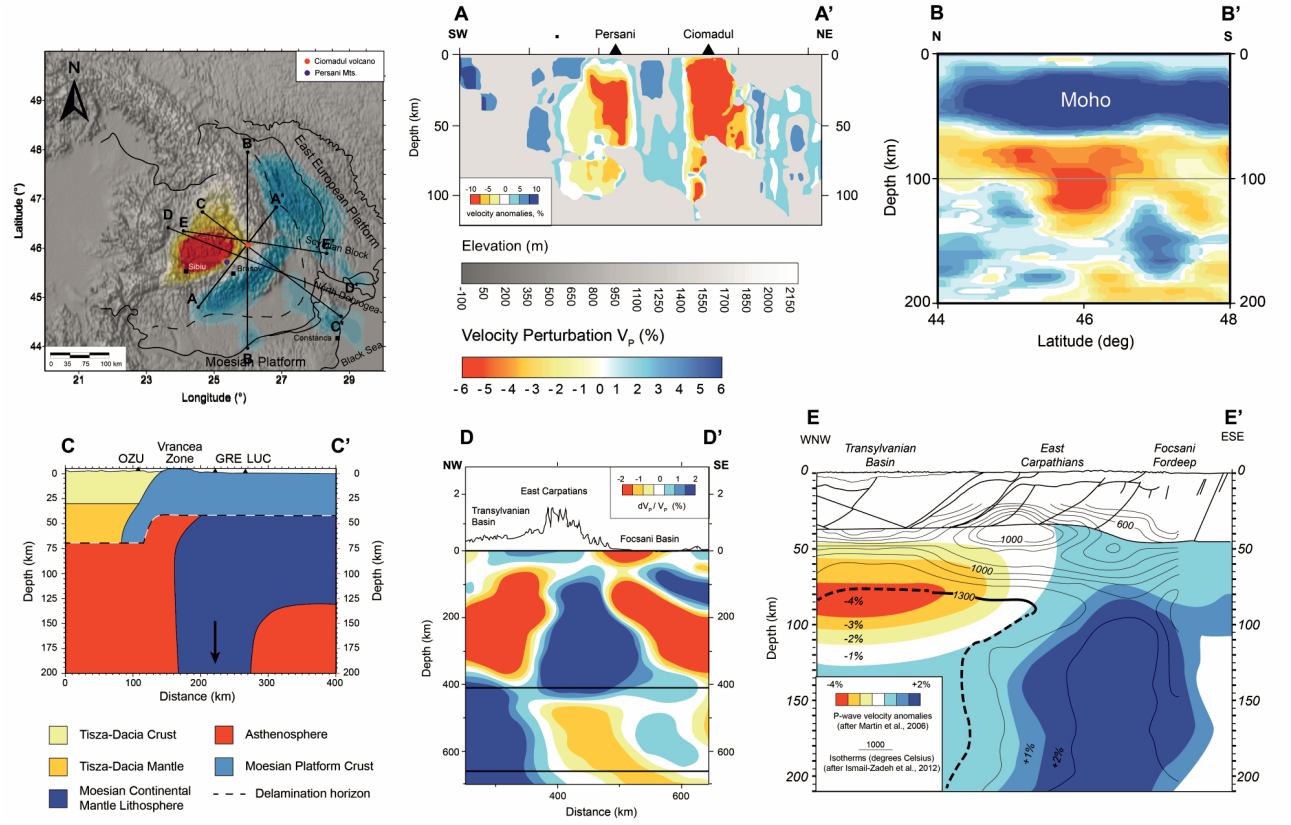

Fig. 5. Different simplified cross-sections on the topographic map show the location of the profiles and integrated results of relative P-wave velocity structure by Martin & Wenzel (2006) at depth slice between 70–100 km; **A–A'** cross-section shows the seismic tomography (S-waves) by Popa et al. (2012); **B–B'** cross-section shows the S-receiver function profile by Kind et al. (2017); **C–C'** cross-section shows the delamination depth of seismic attenuation by Russo et al. (2005); **D–D'** cross-section shows the P-wave tomographic model by Ren et al. (2012); **E–E'** cross-section shows the geometry and thermal structure of the lithosphere by Tiliță et al. (2018).

and tends to escape. The asthenosphere could be effectively channeled eastward into the Carpathian Bend area bounded to the thicker Moeasian and European plates. The squeezed asthenosphere gets blocked by the Vrancea seismogenic body on the SE resulting in its uplift and forces the continuous delamination of the continental lithosphere still attached to the Vrancea Slab (Fig. 5). In this model the asthenosphere is not just responding passively to tectonic movements, but its movement is an active driving force causing uplift in the inner NW part of the Carpathian Bend area and subsidence in the outer SE part through the continuous delamination of the lower lithospheric mantle and forcing it to sink. Toroidal asthenospheric flows generated by the sinking and retreating slab may also contribute to the geodynamic complexity seen in the Carpathian Bend area.

Conclusions

The transitional area between the Pannonian Basin and East Carpathians is characterized by active and complex geotectonic. To fully understand this system behavior, it is essential to understand the melt dynamics and its role in determining the evolution of the system. Defining LAB is a key element in this endeavor. Having this aim in mind and benefiting of the TopoTransylvania initiative (Matenco 2018), a set of new six broadband MT stations were installed on a profile going from Pannonian Basin to East Carpathians.

The new long-period TopoTransylvania MT section demonstrated that the eLAB is the thinnest beneath the Pannonian Basin (~50 km), it thickens at the boundary between the Apuseni Mts. and the Pannonian Basin (~90 km), it is at a constants depth in the Transylvanian Basin (~70–80 km), and the thickest along the East Carpathians (>100 km). In the Carpathian Bend area the eLAB depth decreases to ~80 km again. This shallower depth of the eLAB in this region is in line with independent previous seismic, thermal and MT measurements and could be due to the regional asthenospheric updoming of the area. The asthenospheric updoming is reflected in the young volcanic activity, CO_2-rich surface emanations and springs, active surface and upper mantle deformations in the area. Our results indicate the LAB beneath the Transylvanian Basin is not thick and much thinner than those of the European and Moesian Platforms bordering the Carpathian orogenic belt to the east and south, respectively. The induction arrows indicate the presence of deep well

conductive zones towards the Pannonian Basin, the Bogdan Vodă–Dragoș Vodă fault zone and the East Carpathians. This could be explained by the elevated position of the well conductive asthenosphere in the Pannonian Basin and deep and presumably fluid rich tectonic zones associated with the Bogdan Vodă–Dragoș Vodă fault and the East Carpathians. The phase tensors reveal that the most complex tectonic zones are present in the vicinity of the East Carpathians, which is in line with the relatively young age of the mountain belt, its ongoing geodynamic activity and the very complex nature of collisional orogens.

Acknowledgements: The project was further financed by a Lendület Research Grant to the MTA FI Lendület Pannon LitH_2Oscope Research Group (LP-2018/5), NKFIH K141956 grant to the TopoTransylvania community and NKFIH K116528 and K116604 REvPAMS community.

References

Abt D.L., Fischer K.M., French S.W., Ford H.A., Yuan H. & Romanowicz B. 2010: North American lithospheric discontinuity structure imaged by Ps and Sp receiver functions. *Journal of Geophysical Research Solid Earth* 115, 1–24. https://doi.org/10.1029/2009JB006914

Ádám A. 1965: Einige Hypothesen über den Aufbau des oberen Erdmantel in Ungran. *Gerlands Beiträge zur Geophysik* 74, 20–40.

Ádám A. 1976: Geoelectric and Geothermal Studies. KAPG Geophysical Monograph. Akadémiai Kiadó, 1–772.

Ádám A. & Wesztergom V. 2001: An attempt to map the depth of the electrical asthenosphere by deep magnetotelluric measurements in the Pannonian Basin (Hungary). *Acta Geologica Hungarica* 44, 167–192.

Ádám A., Szarka L., Prácser E. & Varga G. 1996: Mantle plumes or EM distortions in the Pannonian Basin? (Inversion of the deep magnetotelluric (MT) soundings along the Pannonian Geotraverse). *Geofizika Közlemények* 40, 45–78.

Ádám A., Szarka L., Novák A. & Wesztergom V. 2017: Key results on deep electrical conductivity anomalies in the Pannonian Basin (PB), and their geodynamic aspects. *Acta Geodaetica et Geophysica* 52, 205–228. https://doi.org/10.1007/s40328-016-0192-2

Artemieva I.M. 2009: The continental lithosphere: Reconciling thermal, seismic, and petrologic data. *Lithos* 109, 23–46. https://doi.org/10.1016/j.lithos.2008.09.015

Artemieva I.M. & Shulgin A. 2019: Geodynamics of Anatolia: Lithosphere Thermal Structure and Thickness. *Tectonics* 38, 4465–4487. https://doi.org/10.1029/2019TC005594

Aulbach S., Jacob D.E., Cartigny P., Stern R.A., Simonetti S.S., Wörner G.& Viljoen K.S. 2017: Eclogite xenoliths from Orapa: Ocean crust recycling, mantle metasomatism and carbon cycling at the western Zimbabwe craton margin. *Geochimica et Cosmochimica Acta* 213, 574–592. https://doi.org/10.1016/j.gca.2017.06.038

Babuška V. & Plomerová J. 1988: Subcrustal continental lithosphere: a model of its thickness and anisotropic structure. *Physics of the Earth and Planetary Interiors* 51, 130–132. https://doi.org/10.1016/0031-9201(88)90033-7

Babuška V. & Plomerová J. 1992: The lithosphere in central Europe – seismological and petrological aspects. *Tectonophysics* 207, 141–163. https://doi.org/10.1016/0040-1951(92)90475-L

Babuška V. & Plomerová J. 1993: Lithospheric thickness and velocity anisotropy – seismological and geothermal aspects. Tectonophysics 225, 79–89. https://doi.org/10.1016/0040-1951(93)90250-N

Babuška V. & Plomerová J. 2004: The Sorgenfrei–Tornquist Zone as the mantle edge of Baltica lithosphere: new evidence from three-dimensional seismic anisotropy. *Terra Nova* 16, 243–249. https://doi.org/10.1111/j.1365-3121.2004.00558.x

Babuška V. & Plomerová J. 2006: European mantle lithosphere assembled from rigid microplates with inherited seismic anisotropy. *Physics of the Earth and Planetary Interiors* 158, 264–280. https://doi.org/10.1016/j.pepi.2006.01.010

Babuška V., Plomerová J.& Šílený J. 1987: Structural model of the subcrustal lithosphere in central Europe. In: Composition, Structure and Dynamics of the Lithosphere–Asthenosphere System, 239–251. https://doi.org/10.1029/GD016p0239

Bada G., Horváth F., Dövényi P., Szafián P., Windhoffer G.& Cloetingh S. 2007: Present-day stress field and tectonic inversion in the Pannonian basin. *Global and Planetary Change* 58, 165–180. https://doi.org/10.1016/j.gloplacha.2007.01.007

Baron J. & Morelli A. 2017: Full-waveform seismic tomography of the Vrancea, Romania, subduction region. *Physics of the Earth and Planetary Interiors* 273, 36–49. https://doi.org/10.1016/j.pepi.2017.10.009

Belinić T., Stipčević J. & Živčić M. 2018: Lithospheric thickness under the Dinarides. *Earth and Planetary Science Letters* 484, 229–240. https://doi.org/10.1016/j.epsl.2017.12.030

Bibby H.M., Caldwell T.G. & Brown C. 2005: Determinable and non-determinable parameters of galvanic distortion in magnetotellurics. *Geophysical Journal International* 163, 915–930. https://doi.org/10.1111/j.1365-246X.2005.02779.x

Bielik M., Zeyen H., Starostenko V., Makarenko I., Legostaeva O., Savchenko S., Dérerová J., Grinč M., Godová D. & Pánisová J. 2022: A review of geophysical studies of the lithosphere in the Carpathian–Pannonian region. *Geologica Carpathica* 73, 499–516. https://doi.org/10.31577/GeolCarp.73.6.2

Cagniard L. 1953: Basic Theory of the Magneto-Telluric Method of Geophysical Prospecting. *Geophysics* 18, 605–635. https://doi.org/10.1190/1.1437915

Caldwell T.G., Bibby H.M. & Brown C. 2004: The magnetotelluric phase tensor. *Geophysical Journal International* 158, 457–469. https://doi.org/10.1111/j.1365-246X.2004.02281.x

Čermak V. 1993: Lithospheric thermal regimes in Europe. *Physics of the Earth and Planetary Interiors* 79, 179–193. https://doi.org/10.1016/0031-9201(93)90147-2

Ciulavu D., Dinu C., Szakács A. & Dordea D. 2000: Neogene kinematics of the Transylvanian basin (Romania). *American Association of Petroleum Geologists Bulletin* 84, 1589–1615. https://doi.org/10.1306/8626BF0B-173B-11D7-8645000102C1865D

Constable S.C., Parker R.L. & Constable C.G. 1987: Occam's inversion: a practical algorithm for generating smooth models from electromagnetic sounding data. *Geophysics* 52, 289–300. https://doi.org/10.1190/1.1442303

Csontos L. & Nagymarosy A. 1998: The Mid-Hungarian line: a zone of repeated tectonic inversions. *Tectonophysics* 297, 51–71. https://doi.org/10.1016/S0040-1951(98)00163-2

Csontos L. & Vörös A. 2004: Mesozoic plate tectonic reconstruction of the Carpathian region. *Palaeogeography, Palaeoclimatology, Palaeoecology* 210, 1–56. https://doi.org/10.1016/j.palaeo.2004.02.033

Dérerová J., Zeyen H., Bielik M. & Salman K. 2006: Application of integrated geophysical modeling for determination of the continental lithospheric thermal structure in the eastern Carpathians. *Tectonics* 25. https://doi.org/10.1029/2005TC001883

Eaton D.W., Darbyshire F., Evans R.L., Grütter H., Jones A.G. & Yuan X. 2009: The elusive lithosphere-asthenosphere boundary

(LAB) beneath cratons. *Lithos* 109, 1–22. https://doi.org/10.1016/j.lithos.2008.05.009

Egbert G.D. & Booker J.R. 1986: Robust estimation of geomagnetic transfer functions. *Geophysical Journal of the Royal Astronomical Society* 87, 173–194. https://doi.org/10.1111/j.1365-246X.1986.tb04552.x

Egbert G.D. & Livelybrooks D.W. 1996: Single station magnetotelluric impedance estimation: Coherence weighting and the regression M-estimate. *Geophysics* 61, 964–970. https://doi.org/10.1190/1.1444045

Falus G., Tommasi A., Ingrin J. & Szabó C. 2008: Deformation and seismic anisotropy of the lithospheric mantle in the southeastern Carpathians inferred from the study of mantle xenoliths. *Earth and Planetary Science Letters* 272, 50–64. https://doi.org/10.1016/j.epsl.2008.04.035

Fei H., Koizumi S., Sakamoto N., Hashiguchi M., Yurimoto H., Marquardt K., Miyajima N., Yamazaki D. & Katsura T. 2016: New constraints on upper mantle creep mechanism inferred from silicon grain-boundary diffusion rates. *Earth and Planetary Science Letters* 433, 350–359. https://doi.org/10.1016/j.epsl.2015.11.014

Fodor L., Csontos L., Bada G., Györfi I. & Benkovics L. 1999: Tertiary tectonic evolution of the Pannonian Basin system and neighbouring orogens: a new synthesis of palaeostress data. *Geological Society, London, Special Publications* 156, 295–334. https://doi.org/10.1144/GSL.SP.1999.156.01.15

Fullea J. 2017: On Joint Modelling of Electrical Conductivity and Other Geophysical and Petrological Observables to Infer the Structure of the Lithosphere and Underlying Upper Mantle. *Surveys in Geophysics* 38, 963–1004. https://doi.org/10.1007/s10712-017-9432-4

Geissler W.H., Sodoudi F. & Kind R. 2010: Thickness of the central and eastern European lithosphere as seen by S receiver functions. *Geophysical Journal International* 181, 604–634. https://doi.org/10.1111/j.1365-246X.2010.04548.x

GEOSYSTEM SRL. 2008: WinGLink User's Guide. Italy., Release 2.20.02.02.

Girard J., Chen J., Raterron P. & Holyoke C.W. 2013: Hydrolytic weakening of olivine at mantle pressure: Evidence of [100](010) slip system softening from single-crystal deformation experiments. *Physics of the Earth and Planetary Interiors* 216, 12–20. https://doi.org/10.1016/j.pepi.2012.10.009

Green D.H., Hibberson W.O., Kovács I.J. & Rosenthal A. 2010: Water and its influence on the lithosphere-asthenosphere boundary. *Nature* 467, 448–451. https://doi.org/10.1038/nature09369

Gröger H.R., Fügenschuh B., Tischler M., Schmid S.M. & Foeken J.P.T. 2008: Tertiary cooling and exhumation history in the Maramures area (internal eastern Carpathians, northern Romania): Thermochronology and structural data. *Geological Society, London, Special Publications* 298, 169–195. https://doi.org/10.1144/SP298.9

Groom R.W. & Bailey R.C. 1989: Decomposition of magnetotelluric impedance tensors in the presence of local three-dimensional galvanic distortion. *Journal of Geophysical Research Solid Earth* 94, 1913–1925. https://doi.org/10.1029/JB094iB02p01913

Harangi S., Molnár M., Vinkler A.P., Kiss B., Jull A.J.T. & Leonard A.G. 2010: Radiocarbon dating of the last volcanic eruptions of Ciomadul Volcano, southeast carpathians, Eastern-Central Europe. *Radiocarbon* 52, 1498–1507. https://doi.org/10.1017/S0033822200046580

Harangi S., Novák A., Kiss B., Seghedi I., Lukács R., Szarka L., Wesztergom V., Metwaly M. & Gribovszki K. 2015: Combined magnetotelluric and petrologic constrains for the nature of the magma storage system beneath the Late Pleistocene Ciomadul volcano (SE Carpathians). *Journal of Volcanology and Geothermal Research* 290, 82–96. https://doi.org/10.1016/j.jvolgeores.2014.12.006

Heinson G. 1999: Electromagnetic studies of the lithosphere and asthenosphere. *Surveys in Geophysics* 20, 229–255. https://doi.org/10.1023/A:1006689521329

Horváth F. 1993: Towards a mechanical model for the formation of the Pannonian basin. *Tectonophysics* 226, 333–357. https://doi.org/10.1016/0040-1951(93)90126-5

Horváth F., Musitz B., Balázs A., Végh A., Uhrin A., Nádor A., Koroknai B., Pap N., Tóth T. & Wórum G. 2015: Evolution of the Pannonian basin and its geothermal resources. *Geothermics* 53, 328–352. https://doi.org/10.1016/j.geothermics.2014.07.009

Houseman G.A. & Gemmer L. 2007: Intra-orogenic extension driven by gravitational instability: Carpathian–Pannonian orogeny. *Geology* 35, 1135. https://doi.org/10.1130/G23993A.1

Huismans R.S., Bertotti G., Ciulavu D., Sanders C.A.E., Cloetingh S. & Dinu C. 1997: Structural evolution of the Transylvanian Basin (Romania): A sedimentary basin in the bend zone of the Carpathians. *Tectonophysics* 272, 249–268. https://doi.org/10.1016/S0040-1951(96)00261-2

Ismail-Zadeh A., Matenco L., Radulian M., Cloetingh S. & Panza G. 2012: Geodynamics and intermediate-depth seismicity in Vrancea (the south-eastern Carpathians): Current state-of-the art. *Tectonophysics* 530–531, 50–79. https://doi.org/10.1016/j.tecto.2012.01.016

Jackson I., Faul U.H., Suetsugu D., Bina C., Inoue T. & Jellinek M. 2010: Grainsize-sensitive viscoelastic relaxation in olivine: Towards a robust laboratory-based model for seismological application. *Physics of the Earth and Planetary Interiors* 183, 151–163. https://doi.org/10.1016/j.pepi.2010.09.005

Jones A.G. 1999: Imaging the continental upper mantle using electromagnetic methods. *Lithos* 48, 57–80. https://doi.org/10.1016/S0024-4937(99)00022-5

Jones A.G., Plomerova J., Korja T., Sodoudi F. & Spakman W. 2010: Europe from the bottom up: A statistical examination of the central and northern European lithosphere-asthenosphere boundary from comparing seismological and electromagnetic observations. *Lithos* 120, 14–29. https://doi.org/10.1016/j.lithos.2010.07.013

Kalmár D., Petrescu L., Stipčević J., Balázs A. & Kovács I.J. 2023: Lithospheric Structure of the Circum-Pannonian Region Imaged by S-To-P Receiver Functions. *Geochemistry, Geophysics, Geosystems* 24, 9. https://doi.org/10.1029/2023GC010937

Karato S.I. 2012: On the origin of the asthenosphere. *Earth and Planetary Science Letters* 321–322, 95–103. https://doi.org/10.1016/j.epsl.2012.01.001

Karato S.I., Olugboji T. & Park J. 2015: Mechanisms and geologic significance of the mid-lithosphere discontinuity in the continents. *Nature Geoscience* 8, 509–514. https://doi.org/10.1038/ngeo2462

Karátson D., Wulf S., Veres D., Magyari E.K., Gertisser R., Timar G., Novothny A., Telbisz T., Szalai Z., Anechitei-Deacu V., Appelt O., Bormann M., Jánosi C., Hubay K. & Schäbitz F. 2016: The latest explosive eruptions of Ciomadul (Csomád) volcano, East Carpathians – A tephrostratigraphic approach for the 51–29 ka BP time interval. *Journal of Volcanology and Geothermal Research* 319, 29–51. https://doi.org/10.1016/j.jvolgeores.2016.03.005

Karátson D., Telbisz T., Dibacto S., Lahitte P., Szakács A., Veres D., Gertisser R., Jánosi C. & Timár G. 2019: Eruptive history of the Late Quaternary Ciomadul (Csomád) volcano, East Carpathians, part II: magma output rates. *Bulletin of Volcanology* 81. https://doi.org/10.1007/s00445-019-1287-8

Kázmér M. & Kovács S. 1985: Permian–Paleogene paleogeography along the eastern part of the Insubric–Periadriatic lineament system: evidence for continental escape of the Bakony–Drauzug unit. *Acta Geologica Hungarica* 28, 71–84.

Kind R., Handy M.R., Yuan X., Meier T., Kämpf H. & Soomro R. 2017: Detection of a new sub-lithospheric discontinuity in Central Europe with S-receiver functions. *Tectonophysics* 700–701, 19–31. https://doi.org/10.1016/j.tecto.2017.02.002

Kirkby A., Zhang F., Peacock J., Hassan R. & Duan J. 2019: The MTPy software package for magnetotelluric data analysis and visualisation. *The Journal of Open Source Software* 4, 1358. https://doi.org/10.21105/joss.01358

Kis B.M., Caracausi A., Palcsu L., Baciu C., Ionescu A., Futó I., Sciarra A. & Harangi S. 2019: Noble Gas and Carbon Isotope Systematics at the Seemingly Inactive Ciomadul Volcano (Eastern-Central Europe, Romania): Evidence for Volcanic Degassing. *Geochemistry, Geophysics, Geosystems* 20, 3019–3043. https://doi.org/10.1029/2018GC008153

Klébesz R., Gráczer Z., Szanyi G., Liptai N., Kovács I., Patkó L., Pintér Z., Falus G., Wesztergom V. & Szabó C. 2015: Constraints on the thickness and seismic properties of the lithosphere in an extensional setting (Nógrád-Gömör Volcanic Field, Northern Pannonian Basin). *Acta Geodaetica et Geophysica* 50, 133–149. https://doi.org/10.1007/s40328-014-0094-0

Korja T. 2007: How is the European lithosphere imaged by magnetotellurics? *Surveys in Geophysics* 28, 239–272. https://doi.org/10.1007/s10712-007-9024-9

Koroknai B., Wórum G., Tóth T., Koroknai Z., Fekete-Németh V. & Kovács G. 2020: Geological deformations in the Pannonian Basin during the neotectonic phase: New insights from the latest regional mapping in Hungary. *Earth-Science Reviews* 211. https://doi.org/10.1016/j.earscirev.2020.103411

Kovács I.J., Green D.H., Rosenthal A., Hermann J., O'neill H.S.C., Hibberson W.O. & Udvardi B. 2012: An experimental study of water in nominally anhydrous minerals in the upper mantle near the water-saturated solidus. *Journal of Petrology* 53, 2067–2093. https://doi.org/10.1093/petrology/egs044

Kovács I.J., Lenkey L., Green D.H., Fancsik T., Falus G., Kiss J., Orosz L., Angyal J. & Vikor Z. 2017: The role of pargasitic amphibole in the formation of major geophysical discontinuities in the shallow upper mantle. *Acta Geodaetica et Geophysica* 52, 183–204. https://doi.org/10.1007/s40328-016-0191-3

Kovács I.J., Patkó L., Falus G., Aradi L.E., Szanyi G., Gráczer Z. & Szabó C. 2018: Upper mantle xenoliths as sources of geophysical information: the Perşani Mts. area as a case study. *Acta Geodaetica et Geophysica* 53, 415–438. https://doi.org/10.1007/s40328-018-0231-2

Kovács I.J., Liptai N., Koptev A., Cloetingh S.A.P.L., Lange T.P., Maţenco L., Szakács A., Radulian M., Berkesi M., Patkó L., Molnár G., Novák A., Wesztergom V., Szabó C. & Fancsik T. 2021: The 'pargasosphere' hypothesis: Looking at global plate tectonics from a new perspective. *Global and Planetary Change* 204. https://doi.org/10.1016/j.gloplacha.2021.103547

Krézsek C. & Bally A.W. 2006: The Transylvanian Basin (Romania) and its relation to the Carpathian fold and thrust belt: Insights in gravitational salt tectonics. *Marine and Petroleum Geology* 23, 405–442. https://doi.org/10.1016/j.marpetgeo.2006.03.003

Lange T.P., Szabó C., Liptai N., Patkó L., Gelencsér O., Aradi L.E. & Kovács I.J. 2019: Rheology study on the earth's mantle: Application of quantitative Fourier transform infrared spectroscopyon upper mantle xenolith from the Perşani Mountains (in Hungarian). *Földtani Közlöny* 149, 233. https://doi.org/10.23928/foldt.kozl.2019.149.3.233

Lange T.P., Palcsu L., Szakács A., Kővágó Á., Gelencsér O., Gál Á., Gyila S., M. Tóth T., Maţenco L., Krézsek C., Lenkey L., Szabó C. & Kovács I.J. 2023: The link between lithospheric scale deformations and deep fluid emanations: Inferences from the Southeastern Carpathians, Romania. *Evolving Earth* 1, 100013. https://doi.org/10.1016/j.eve.2023.100013

Ledo J. & Jones A.G. 2005: Upper mantle temperature determined from combining mineral composition, electrical conductivity laboratory studies and magnetotelluric field observations: Application to the intermontane belt, Northern Canadian Cordillera. *Earth and Planetary Science Letters* 236, 258–268. https://doi.org/10.1016/j.epsl.2005.01.044

Leever K.A., Matenco L., Bertotti G., Cloetingh S. & Drijkoningen G.G. 2006: Late orogenic vertical movements in the Carpathian Bend Zone–seismic constraints on the transition zone from orogen to foredeep. *Basin Research* 18, 521–545.

Lenkey L., Mihályka J. & Paróczi P. 2021: Review of geothermal conditions of Hungary. *Földtani Közlöny* 151, 65. https://doi.org/10.23928/foldt.kozl.2021.151.1.65

Linzer H.G., Frisch W., Zweigel P., Girbacea R., Hann H.P. & Moser F. 1998: Kinematic evolution of the Romanian Carpathians. *Tectonophysics* 297, 133–156. https://doi.org/10.1016/S0040-1951(98)00166-8

Liptai N., Gráczer Z., Szanyi G., Cloetingh S., Süle B., Aradi L.E., Falus G., Bokelmann G., Timkó M., Timár G., Szabó C. & Kovács I.J. 2022: Seismic anisotropy in the mantle of a tectonically inverted extensional basin: a shear-wave splitting and mantle xenolith study on the western Carpathian-Pannonian region. *Tectonophysics* 845, 229643. https://doi.org/10.1016/j.tecto.2022.229643

Martin M. & Wenzel F. 2006: High-resolution teleseismic body wave tomography beneath SE-Romania – II. Imaging of a slab detachment scenario. *Geophysical Journal International* 164, 579–595. https://doi.org/10.1111/j.1365-246X.2006.02884.x

Márton E. 1987: Palaeomagnetism and tectonics in the Mediterranean region. *Journal of Geodynamics* 7, 33–57.

Matenco L. 2018: Topo-Transylvania: a multidisciplinary Earth science initiative in Central Europe to tackle local and global challenges. *Acta Geodaetica et Geophysica* 53, 323–329. https://doi.org/10.1007/s40328-018-0234-z

McKenzie D. 1978: Some remarks on the development of sedimentary basins. *Earth and Planetary Science Letters* 40, 25–32. https://doi.org/10.1016/0012-821X(78)90071-7

Molnár K., Lukács R., Dunkl I., Schmitt A.K., Kiss B., Seghedi I., Szepesi J. & Harangi S. 2019: Episodes of dormancy and eruption of the Late Pleistocene Ciomadul volcanic complex (Eastern Carpathians, Romania) constrained by zircon geochronology. *Journal of Volcanology and Geothermal Research* 373, 133–147. https://doi.org/10.1016/j.jvolgeores.2019.01.025

Niu Y. & Green D.H. 2018: The petrological control on the lithosphere–asthenosphere boundary (LAB) beneath ocean basins. *Earth-Science Reviews* 185, 301–307. https://doi.org/10.1016/j.earscirev.2018.06.011

Panaiotu C.G., Jicha B.R., Singer B.S., Ţugui A., Seghedi I., Panaiotu A.G. & Necula C. 2013: $^{40}Ar/^{39}Ar$ chronology and paleomagnetism of Quaternary basaltic lavas from the Perşani Mountains (East Carpathians). *Physics of the Earth and Planetary Interiors* 221, 1–14. https://doi.org/10.1016/j.pepi.2013.06.007

Parkinson W.D. 1959: Directions of rapid geomagnetic fluctuations. *Geophysical Journal International* 2, 1–14. https://doi.org/10.1111/j.1365-246X.1959.tb05776.x

Pécskay Z., Lexa J., Balogh K., Szakács A., Seghedi I., Konečný V., Kovács M., Márton E., Kaliciak M., Széky-Fux V., Póka T., Gyarmati P., Edelstein O., Rosu E. & Zec B. 1995: Space and time distribution of Neogene–Quarternary volcanism in the Carpatho–Pannonian Region. *Acta Vulcanology Special Issue* 7, 15–28.

Pécskay Z., Lexa J., Szakács A., Seghedi I., Balogh K., Konečný V., Zelenka T., Kovacs M., Póka T., Fülöp A., Márton E., Panaiotu C. & Cvetković V. 2006: Geochronology of Neogene magmatism in the Carpathian arc and intra-Carpathian area. *Geolgica Carpathica* 57, 511–530.

Petrescu L., Stuart G., Houseman G. & Bastow I. 2020: Upper mantle deformation signatures of craton-orogen interaction in the Carpathian–Pannonian region from SKS anisotropy analysis. *Geophysical Journal International* 220, 2105–2118. https://doi.org/10.1093/gji/ggz573

Plomerová J. & Babuška V. 2010: Long memory of mantle lithosphere fabric – European LAB constrained from seismic anisotropy. *Lithos* 120, 131–143. https://doi.org/10.1016/j.lithos.2010.01.008

Plomerová J., Babuška V., Vecsey L. & Kouba D. 2002a: Seismic anisotropy of the lithosphere around the Trans-European Suture Zone (TESZ) based on teleseismic body-wave data of the TOR experiment. *Tectonophysics* 360, 89–114. https://doi.org/10.1016/S0040-1951(02)00349-9

Plomerová J., Kouba D. & Babuška V. 2002b: Mapping the lithosphere–asthenosphere boundary through changes in surface-wave anisotropy. *Tectonophysics* 358, 175–185. https://doi.org/10.1016/S0040-1951(02)00423-7

Plomerová J., Babuška V., Vecsey L., Kozlovskaya E., Raita T., Achauer U., Alinaghi A., Ansorge J., Bock G., Bruneton M., Friederich W., Grad M., Guterch A., Heikkinen P., Hjelt S.E., Hyvonen T., Isanina E., Kissling E., Komminaho K., Korja A., Nevsky M. V., Pavlenkova N.I., Pedersen H., Riznichenko O.Y., Roberts R.G., Sandoval S., Sanina I.A., Sharov N. V., Tiikkainen J., Volosov S.G., Wieland E., Wylegalla K., Yliniemi J. & Yurov Y. 2006: Proterozoic–Archean boundary in the mantle lithosphere of eastern Fennoscandia as seen by seismic anisotropy. *Journal of Geodynamics* 41, 400–410. https://doi.org/10.1016/j.jog.2005.10.008

Pollack H.N. & Chapman D.S. 1977: On the regional variation of heat flow, geotherms, and lithospheric thickness. *Tectonophysics* 38, 279–296. https://doi.org/10.1016/0040-1951(77)90215-3

Popa M., Radulian M., Grecu B., Popescu E. & Placinta A.O. 2005: Attenuation in Southeastern Carpathians area: Result of upper mantle inhomogeneity. *Tectonophysics* 410, 235–249. https://doi.org/10.1016/j.tecto.2004.12.037

Popa M., Radulian M., Szakács A., Seghedi I. & Zaharia B. 2012: New Seismic and Tomography Data in the Southern Part of the Harghita Mountains (Romania, Southeastern Carpathians): Connection with Recent Volcanic Activity. *Pure and Applied Geophysics* 169, 1557–1573. https://doi.org/10.1007/s00024-011-0428-6

Posgay K., Bodoky T., Hegedüs E., Kovácsvölgyi S., Lenkey L., Szafián P., Takács E., Tímár Z. & Varga G. 1995: Asthenospheric structure beneath a Neogene basin in southeast Hungary. *Tectonophysics* 252, 467–484. https://doi.org/10.1016/0040-1951(95)00098-4

Praus O., Pěčová J., Petr V., Babuška V. & Plomerová J. 1990: Magnetotelluric and seismological determination of the lithosphere-asthenosphere transition in Central Europe. *Physics of the Earth and Planetary Interiors* 60, 212–228. https://doi.org/10.1016/0031-9201(90)90262-V

Radulian M., Popa M., Cărbunar O. & Rogozea M. 2008: Seismicity patterns in Vrancea and predictive features. *Acta Geodaetica et Geophysica Hungarica* 43, 163–173. https://doi.org/10.1556/AGeod.43.2008.2-3.6

Ratschbacher L., Linzer H., Moser F., Strusievicz R., Bedelean H., Har N. & Mogoş P. 1993: Cretaceous to Miocene thrusting and wrenching along the central south Carpathians due to a corner effect during collision and orocline formation. *Tectonics* 12, 855–873. https://doi.org/10.1029/93TC00232

Ren Y., Stuart G.W., Houseman G.A., Dando B., Ionescu C., Hegedüs E., Radovanović S. & Shen Y. 2012: Upper mantle structures beneath the Carpathian-Pannonian region: Implications for the geodynamics of continental collision. *Earth and Planetary Science Letters* 349–350, 139–152. https://doi.org/10.1016/j.epsl.2012.06.037

Ren Y., Grecu B., Stuart G., Houseman G.A., Dando B., Lorinczi P., Gogus O., Hegedüs E., Kovács A., Török I., László I., Csabafi R., Ionescu C., Radulian M., Raileanu V., Tataru D., Zaharia B., Borleanu F., Neagoe C., Gainariu G., Rau D., Radovanovic S., Kovacevic V., Valcic D., Petrovic-Cacic S., Krunic G., Brisbourne A. & Hawthorn D., Lane V. 2013: Crustal structure of the Carpathian–Pannonian region from ambient noise tomography. *Geophysical Journal International* 195, 1351–1369. https://doi.org/10.1093/gji/ggt316

Royden L., Horváth F., Nagymarosy A. & Stegena L. 1983: Evolution of the Pannonian Basin System: 2. Subsidence and thermal history. *Tectonics* 2, 91–137. https://doi.org/10.1029/TC002i001p00091

Rubóczki T., Novák A., Liptai N., Porkoláb K., Molnár C., Galsa A., Molnár G., Wesztergom V. & Kovács I.J. 2024: The Pannon LitH_2Oscope magnetotelluric array in the Pannonian Basin. *Acta Geodaetica et Geophysica*. https://doi.org/10.1007/s40328-024-00434-1

Russo R.M., Mocanu V., Radulian M., Popa M. & Bonjer K.P. 2005: Seismic attenuation in the Carpathian bend zone and surroundings. *Earth and Planetary Science Letters* 237, 695–709. https://doi.org/10.1016/j.epsl.2005.06.046

Rychert C.A., Harmon N., Constable S. & Wang S. 2020: The nature of the lithosphere–asthenosphere boundary. *Journal of Geophysical Research Solid Earth* 125, e2018JB016463. https://doi.org/10.1029/2018JB016463

Saha S., Dasgupta R. & Tsuno K. 2018: High Pressure Phase Relations of a Depleted Peridotite Fluxed by CO_2-H_2O-Bearing Siliceous Melts and the Origin of Mid-Lithospheric Discontinuity. *Geochemistry, Geophysics, Geosystems* 19, 595–620. https://doi.org/10.1002/2017GC007233

Samae V., Cordier P., Demouchy S., Bollinger C., Gasc J., Koizumi S., Mussi A., Schryvers D. & Idrissi H. 2021: Stress-induced amorphization triggers deformation in the lithospheric mantle. *Nature* 591, 82–86. https://doi.org/10.1038/s41586-021-03238-3

Săndulescu M., Visarion M., Stanica D., Stanica M. & Atanasiu L. 1993: Deep Structure of the inner Carpathians in the Maramures–Tisa zone (East Carpathians). *Romanian Journal of Geophysics* 16, 67–76.

Schmid S.M., Bernoulli D., Fügenschuh B., Matenco L., Schefer S., Schuster R., Tischler M. & Ustaszewski K. 2008: The Alpine–Carpathian–Dinaridic orogenic system: Correlation and evolution of tectonic units. *Swiss Journal of Geosciences* 101, 139–183. https://doi.org/10.1007/s00015-008-1247-3

Seghedi I., Downes H., Szakács A., Mason P.R.D., Thirlwall M.F., Emilian R., Pécskay Z., Márton E. & Panaiotu C. 2004: Neogene–Quaternary magmatism and geodynamics in the Carpathian–Pannonian region: A synthesis. *Lithos* 72, 117–146. https://doi.org/10.1016/j.lithos.2003.08.006

Selway K., Yi J. & Karato S.I. 2014: Water content of the Tanzanian lithosphere from magnetotelluric data: Implications for cratonic growth and stability. *Earth and Planetary Science Letters* 388, 175–186. https://doi.org/10.1016/j.epsl.2013.11.024

Selway K., Ford H. & Kelemen P. 2015: The seismic mid-lithosphere discontinuity. *Earth and Planetary Science Letters* 414, 45–57. https://doi.org/10.1016/j.epsl.2014.12.029

Sibson R. 1981: A Brief Description of Natural Neighbor Interpolation. In: Barnett V. (Ed.): Interpreting Multivariate Data. *John Wiley & Sons*, New York, 21–36.

Sifré D., Gardés E., Massuyeau M., Hashim L., Hier-Majumder S. & Gaillard F. 2014: Electrical conductivity during incipient melting in the oceanic low-velocity zone. *Nature* 508, 81–85. https://doi.org/10.1038/nature13245

Stănică M. 1993: An electrical resistivity lithospheric model in the Carpathian Orogen from Romania. *Physics of the Earth and Planetary Interiors* 81, 99–105. https://doi.org/10.1016/0031-9201(93)90126-T

Stănică M., Stănică D. & Marin-Furnică C. 1999: The placement of the Trans-European Suture zone on the Romanian territory by electromagnetic arguments. *Earth, Planets and Space* 51, 1073–1078. https://doi.org/10.1186/BF03351581

Stegena L., Géczy B. & Horváth F. 1975: Late Cenozoic evolution of the Pannonian basin. *Tectonophysics* 26, 71–90. https://doi.org/10.1016/0040-1951(75)90114-6

Szabó C., Harangi S. & Csontos L. 1992: Review of Neogene and Quaternary volcanism of the Carpathian-Pannonian region. *Tectonophysics* 208, 243–256. https://doi.org/10.1016/0040-1951(92)90347-9

Szakács A., Pécskay Z. & Gál Á. 2018: Patterns and trends of time–space evolution of Neogene volcanism in the Carpathian–Pannonian region: a review. *Acta Geodaetica et Geophysica* 53, 347–367. https://doi.org/10.1007/s40328-018-0230-3

Tămaș D.M., Tămaș A., Barabasch J., Rowan M.G., Schleder Z., Krézsek C. & Urai J.L. 2021: Low-Angle Shear Within the Exposed Mânzălești Diapir, Romania: Salt Decapitation in the Eastern Carpathians Fold-and-Thrust Belt. *Tectonics* 40. https://doi.org/10.1029/2021TC006850

Tari G., Dövényi P., Dunkl I., Horváth F., Lenkey L., Stefanescu M., Szafián P. & Tóth T. 1999: Lithospheric structure of the Pannonian basin derived from seismic, gravity and geothermal data. *Geological Society, London, Special Publications* 156, 215–250. https://doi.org/10.1144/GSL.SP.1999.156.01.12

Tesauro M., Hollenstein C., Egli R., Geiger A. & Kahle H.G. 2006: Analysis of central western Europe deformation using GPS and seismic data. *Journal of Geodynamics* 42, 194–209. https://doi.org/10.1016/j.jog.2006.08.001

Tesauro M., Kaban M.K. & Cloetingh S. 2009: A new thermal and rheological model of the European lithosphere. *Tectonophysics* 476, 478–495. https://doi.org/10.1016/j.tecto.2009.07.022

Thybo H. 2006: The heterogeneous upper mantle low velocity zone. *Tectonophysics* 416, 53–79. https://doi.org/10.1016/j.tecto.2005.11.021

Tikhonov A.N. 1950: On determination of electric characteristics of deep layers of the earth's crust. *Doklady* 73, 295–297.

Tiliță M., Lenkey L., Mațenco L., Horváth F., Surányi G. & Cloetingh S. 2018: Heat flow modelling in the Transylvanian basin: Implications for the evolution of the intra-Carpathians area. *Global and Planetary Change* 171, 148–166. https://doi.org/10.1016/j.gloplacha.2018.07.007

Tischler M., Gröger H.R., Fügenschuh B. & Schmid S.M. 2007: Miocene tectonics of the Maramures area (Northern Romania): Implications for the Mid-Hungarian fault zone. *International Journal of Earth Sciences* 96, 473–496. https://doi.org/10.1007/s00531-006-0110-x

Tischler M., Matenco L., Filipescu S., Gröger H.R., Wetzel A. & Fügenschuh B. 2008: Tectonics and sedimentation during convergence of the ALCAPA and Tisza–Dacia continental blocks: The Pienide nappe emplacement and its foredeep (N. Romania). *Geological Society, London, Special Publications* 298, 317–334. https://doi.org/10.1144/SP298.15

Tondi R., Achauer U., Landes M., Daví R. & Besutiu L. 2009: Unveiling seismic and density structure beneath the Vrancea seismogenic zone, Romania. *Journal of Geophysical Research Solid Earth* 114, 1–17. https://doi.org/10.1029/2008JB005992

Vaselli O., Downes H., Thirlwall M., Dobosi G., Coradossi N., Seghedi I., Szakács A. & Vannucci R. 1995: Ultramafic Xenoliths in Plio–Pleistocene Alkali Basalts from the Eastern Transylvanian Basin: Depleted Mantle Enriched by Vein Metasomatism. *Journal of Petrology* 36, 23–53. https://doi.org/10.1093/petrology/36.1.23

Wenzel F., Lorenz F.P., Sperner B. & Oncescu M.C. 1999: Seismotectonics of the Romanian Vrancea Area. In: Vrancea Earthquakes: Tectonics, Hazard and Risk Mitigation, 15–25. https://doi.org/10.1007/978-94-011-4748-4_2

Wiese H. 1962: Geomagnetische Tiefentellurik Teil II: Die Streichrichtung der untergrundstrukturen des elektrischen Widerstandes, erschlossen aus geomagnetischen Variationen. *Geofisica Pura e Applicata* 52, 83–103. https://doi.org/10.1007/BF01996002

Wortel M.J.R. & Spakman W. 2000: Subduction and Slab Detachment in the Mediterranean–Carpathian Region. *Science* 290, 1910–1917. https://doi.org/10.1126/science.290.5498.1910

Xu Y., Shankland T.J. & Duba A.G. 2000: Pressure effect on electrical conductivity of mantle olivine. *Physics of the Earth and Planetary Interiors* 118, 149–161. https://doi.org/10.1016/S0031-9201(99)00135-1

Electronic supplementary material is available online:

Supplementary Fig. S1: The TopoTransylvania MT section (HU24A_MT, LABMT1, LABMT2, LABMT3, LABMT4, LABMT5, LABMT6, CSB6) apparent resistivity and phase soundings, the lines are the original MT data, and the dots represent the decomposed MT soundings. http://geologicacarpathica.com/data/files/supplements/GC-75-3-Novak_FigS1.jpg

Supplementary Fig. S2: The TopoTransylvania MT section 1D inversion result on the decomposed MT soundings invariant mode. The green color model represents the simple layered resistivity model, the green continuous lines are the fitted soundings. The Occam layered model is the wide black line, still, the narrow continuous line is the Bostick depth transformation model of the decomposed MT soundings. http://geologicacarpathica.com/data/files/supplements/GC-75-3-Novak_FigS2.jpg